Published in final edited form as:
Photochem Photobiol Sci. 2014 March ; 13(3): 531–540. doi:10.1039/c3pp50351h.

Grp1-associated scaffold protein regulates skin homeostasis after ultraviolet irradiation

Anand Venkataraman[1,2,§], **Daniel J. Coleman**[1,2], **Daniel J. Nevrivy**[1,2,¶], **Tulley Long**[1,†], **Chrissa Kioussi**[1,2,3], **Arup K. Indra**[1,2,3,4,*], and **Mark Leid**[1,2,5,*]

[1]Department of Pharmaceutical Sciences, Oregon State University, Corvallis, Oregon 97331

[2]Molecular & Cellular Biology Program, Oregon State University, Corvallis, Oregon 97331

[3]Environmental Health Science Center, Oregon State University, Corvallis, Oregon 97331

[4]Department of Dermatology, Oregon Health and Science University, Portland, Oregon, 97239 USA

[5]Department of Integrative Biosciences, Oregon Health and Science University, Portland, Oregon, 97239 USA

Abstract

Grp1-associated scaffold protein (Grasp), the product of a retinoic acid-induced gene in P19 embryonal carcinoma cells, is expressed primarily in brain, heart, and lung of the mouse. We report herein that *Grasp* transcripts are also found in mouse skin in which the *Grasp* gene is robustly induced following acute ultraviolet-B (UVB) exposure. *Grasp*$^{-/-}$ mice were found to exhibit delayed epidermal proliferation and a blunted apoptotic response after acute UVB exposure. Immunohistochemical analyses revealed that the nuclear residence time of the tumor suppressor protein p53 was reduced in *Grasp*$^{-/-}$ mice after UVB exposure. Taken together, our results suggest that a physiological role of Grasp may be to regulate skin homeostasis after UVB exposure, potentially by influencing p53-mediated apoptotic responses in skin.

Introduction

Expression of the *Grasp* gene is induced by treatment of P19 embryonal carcinoma cells with all-*trans* retinoic acid[1]. Grasp was subsequently recloned and referred to as Tamalin[2]. Grasp serves as a molecular scaffold for numerous proteins, including kinases (syk)[3] and guanine nucleotide exchange factors (Grp1, ARNO)[1], and has been shown to regulate the trafficking of membrane receptors, such as mGluR1, and TrkCT1[2, 4, 5]. More recently we showed that trafficking of membrane receptors by Grasp was mediated through its interaction with Grp1 and occurred through the non-clathrin, Arf6-dependent trafficking

Correspondence: Mark Leid, Telephone: 541-737-5809; Telefax: 541-737-3999; Mark.Leid@oregonstate.edu; Arup Indra, Telephone: 541-737-5801; Telefax: 541-737-3999; Arup.Indra@oregonstate.edu.
[§]Present addresses Department of Pharmacology, University of Pennsylvania School of Medicine, 3400 Civic Center Blvd., Bld 421, STRC, Philadelphia, PA 19104.
[¶]Nevrivy Patent Law Group P.L.L.C., 1055 Thomas Jefferson Ave., N.W Suite M-100, Washington D.C. 20007.
[†]Program in the History of Medicine, MMC 506 Mayo Memorial Building, 420 Delaware St. SE, Minneapolis, MN 55455.

pathway[6]. *Grasp* is expressed in post-natal brain, liver, and lung in the mouse[1–3]. Mice lacking *Grasp* exhibit no gross morphological or behavioral deficits, and mildly altered response to morphine and cocaine[7]. Recent studies suggest a role of *Grasp* in hippocampal neurogenesis after a electroconvulsive insult[8], and in dendritic outgrowth/arborization in rat neuronal culture[9]. However the *in vivo* role of *Grasp* remains poorly characterized.

Skin is an excellent system to study proliferative paradigms in response to either chemical stressors, such as ATRA[10, 11], TPA/DMBA[12], or physical stressors, such as ultraviolet (UV) radiation[13–17]. Mouse skin is composed of three primary layers – the outermost epidermis, the underlying dermis, and the innermost layer, the hypodermis. The epidermis is further stratified into the progressively external basal, spinous, granular, and cornified layers[18]. In response to chemical or physical stressors a robust hyperproliferation of basal keratinocytes and thickening of differentiated suprabasal (spinous and granular) layers ensues, which is termed epidermal hyperplasia.

Two apoptotic pathways of physiologic importance have been identified in skin. The first pathway is important during keratinization and the homeostatic process of hair growth in skin[19]. Apoptosis in skin can also be triggered by the tumor suppressor p53 in response to injury, such as exposure to UV radiation[19]. Acute UVB exposure induces cellular damage, most of which disappears within 2 weeks, whereas chronic and repeated exposures result in epidermal cell damage leading to skin cancer[14]. At the molecular level, skin cancers are strongly correlated with *p53* mutations[20] and/or dysregulation of the p53 protein[21]. Following UVB exposure, p53 becomes activated, translocates to the nucleus, and induces expression of target genes leading to cell-cycle arrest with activation of DNA repair pathways or to cell death by activation of the p53-dependent apoptotic pathway[14, 16, 19, 21].

In this study, we report the generation of a *Grasp* knockout mouse (*Grasp*$^{-/-}$) and explore the *in vivo* role of *Grasp* in adult mouse skin. *Grasp* transcripts were found in the epidermal layers of mouse skin and robust induction of *Grasp* gene was noted in both epidermal and dermal layers following acute UVB exposure. *Grasp*$^{-/-}$ mice were found to exhibit delayed epithelial proliferation and a blunted apoptotic response, and reduced nuclear residence time of p53 after acute UVB exposure. Taken together, our results suggest that Grasp is involved in p53-mediated apoptotic signaling following UVB exposure in skin.

Material and Methods

Animals

Grasp$^{-/-}$ animals had been backcrossed with C57BL/6 strain of mice for at least 5 generations before being used in experiments. Two to three month-old male *Grasp*$^{-/-}$ (n = 15) and littermate controls (n = 15) mice were fed a commercial diet and provided with water ad libitum. Mice were maintained in a temperature and humidity-controlled facility with a 12-hour light/dark cycle. All procedures involving animals were carried with prior approval by the Institutional Animal Care and Use Committee at Oregon State University.

Antibodies

Antibodies and dilutions used: anti-p53 (Leica Biosystems Novacastra #NCL-p53-CM5p, 1:500 for IHC; Calbiochem #OP29, 5 μg/ml for immunoblots), anti-Grasp (1:3000; previously described in Ref. [1]), anti-BrdU (1:100, #1370030, AbD Serotec), and anti-β-actin (1:5000, #A5441, Sigma-Aldrich). Antibodies for differentiation markers were purchased from Covance: anti-K14 (1:500; #PRB-155P), anti-K10 (1:500; #PRB-159P), anti-Filaggrin (1:250; #PRB-417P), anti-Loricrin (1:500; #PRB-145P). An anti-Ctip2/Bcl11b antibody (#ab18465 Abcam; 1:2000) was used as a control.

UVB treatment and sample collection

The dorsal hair of mice was shaved 24 hrs prior to UVB exposure to ensure synchronization of the hair-growth cycle[22–24] and to facilitate maximum exposure to the UVB irradiation. Mice were placed on a shelf 20 cm below the light source in standard cages. Mice were irradiated with a single, acute dose of 7.5 kJ/m^2 from a bank of four UVB sunlamps (#TL-40W, Philips) as described previously[25]. Sunlamp irradiance was measured with a model L1400A radiometer/photometer with a SL021/FQI detector (International Light, Inc., Newburyport, MA). Mice were euthanized at 24 and 48 hrs after UV radiation. Biopsies (5 mm^2) from the dorsal skin from each group of mice were collected and either immediately fixed in 4% buffered paraformaldehyde (PFA) or stored in −80°C for future analyses. Control mice (n = 3), which were not exposed to UV, were similarly processed.

Primary fibroblast culture

Primary skin fibroblasts were cultured by removing dorsal and ventral skin from newborn mouse pups and incubating in growth medium containing 5 mg/mL dispase at 4°C overnight with rocking. Skin was washed in sterile PBS on the following day and the epidermis separated and discarded. The dermis was incubated in TrypLE Express (Life Technologies) for 30 min. at 37°C. The dermis was shredded using forceps, suspended in growth medium (F-12 nutrient mixture [Ham], 8% FBS and 1X antibiotic/antimycotic), and vortexed for 2–3 minutes to disperse individual cells. The cell suspension was centrifuged (300 × g, 3 min.) and the pellet was resuspended in fresh growth medium and plated. Medium was changed the day after plating, and cells were split at a 1:5 ratio when confluency was reached. Cells were maintained for several passages by culturing in aforementioned growth medium and using a 1:5 split ratio. All cell culture was performed at 37°C and in 5% CO_2.

UVB treatment of cells

Prior to UVB exposure, cells were washed briefly with sterile PBS and then the PBS was removed by aspiration. Culture dishes with lids removed were then exposed to a single dose of 10 mJ/cm^2 of UVB light from a bank of four Philips FS-40 UV sunlamps. The irradiance of the sunlamps was measured with an IL-1400A radiometer with an SEE240 UVB detector (International Light). Immediately after UVR, fresh growth medium was added back and the cells were returned to the growth incubator.

Immunoblot analysis

Skin samples were homogenized and lysed in a denaturing buffer (250 mM NaCl, 2 mM EDTA, 50 mM NaF, 5mM sodium pyrophosphate, 5mM NEM, 0.1 mM hemin chloride, a protease inhibitor cocktail [leupeptin, aporotinin, bestatin], and 1% SDS), boiled for 5 min., sonicated, and clarified by centrifugation.

Histological and immunohistochemical analysis

Skin samples were fixed in 4% PFA, cryopreserved in 30% sucrose, and frozen in OCT. Cross-sections of 10 μm thickness were prepared and rinsed with PBS three times, and then processed for histological analyses by hematoxylin and eosin (H&E) staining as described previously[26]. Immunohistochemical analyses were carried out as described previously[27]. All fluorescence images (unless mentioned otherwise) were captured using a ZEISS LSM 510 confocal microscope using a 40× Plan Apo objective and bright-field images were captured using the Zeiss Imager.Z1 microscope with a 20× objective. Images were processed using the Zeiss LSM image browser and Photoshop CS4 (Adobe Systems, Inc.). Post-process scoring of $BrdU^+$ and $p53^+$ epidermal cells was performed on 8–10 representative tissue sections from each animal at each time point by blinded individuals.

TUNEL assay

The Promega Dead-end colorimetric kit (#TB199) was used to visualize apoptotic cells in the tissue samples using the manufacturer's protocol with minor modifications: a fluorescent Cy3 flurophore conjugated to streptavidin (SA) was used instead of the colorimetric SA-HRP-DAB visualization procedure.

In situ hybridization

A full-length, *Grasp* cRNA probe, labeled with digoxigenin-dUTP, was generated using Roche's DIG RNA labeling kit (catalog number 11175025910). Tissue preparation and hybridizations were conducted using common techniques. Briefly, 10 μm cryosections were collected on slides and incubated in 4% PFA followed by an incubation with proteinase K (10 mg/ml) for 20 minutes at 25°C. The sections were rinsed and briefly fixed again with 4% PFA. These sections were acetylated in triethanolamine/acetic anhydride for 10 min, and hybridized with the DIG-labelled probe (10 ng/ml) at 65°C. DIG-labeled RNA was visualized using anti-DIG Fab fragments conjugated to alkaline phosphatase (AP) (1:5000; Roche #1093274150) and AP-substrate BM-purple (Roche #1442074).

Quantitative PCR (RT-qPCR) analyses

RNA extraction and cDNA preparation were performed as described[26]. RT-qPCR was performed on an ABI 7500 Real-Time PCR system using SYBR green and analyzed as described[26, 28]. Two sets of *Grasp* primers were used for qPCR, and both sets yielded similar results. Primer sequences for amplification of Grasp were, Primer set 1: (F) 5′-AGCACTGGAGGACTATCAC, (R) 5′-CGAGATCCAGACA-TATGGC; Primer set 2: (F) 5′ - CTCAGGATTCCGTTGGAAGAA-3′; (R) 5′-TTCATGAACT-CGGCAGACGAA-3′.

Statistical analyses

A 2-tailed t-test was performed to determine if the difference between means of two groups was statistically significant. For comparison of three or more groups, values from control and experimental groups were compared using a two-way ANOVA followed by Bonferroni post-hoc analysis.

Results

Generation of *Grasp*$^{-/-}$ mice

A *Grasp* targeting vector was constructed using ~9 kb of the *Grasp* genomic locus (Figs. 1A, B). After electroporation of the *Grasp* targeting vector into ES cells derived from 129/Sv strain of mice, two ES cell lines (out of 113) were verified to have undergone homologous recombination (HR) as judged by analyses using 5′ and 3′ probes (Figs. 1C, D). Both clones were injected into blastocysts, which gave rise to three C57BL6/SV129 chimeric founder animals that were backcrossed C57BL/6 mice for germ line transmission of the targeted L2F2 allele (Fig. S1). We found no phenotypic difference between the three lines and only one was maintained for further studies. Transgenic mice expressing Flp recombinase under control of the CMV promoter[29] were crossed with *Grasp* L2F2 mice to excise the Frt-flanked neomycin marker and generate the L2 (floxed) *Grasp* allele (Fig. S1). Subsequently, mice harboring the L2 allele (LoxP-Exon 1-LoxP) were crossed with transgenic mice expressing Cre recombinase under the control of the protamine promoter[30], to excise the floxed exon 1 of *Grasp* in spermatocytes (Fig. S1). Offspring of these mice were bred to homozygosity (*Grasp*$^{L-/L-}$, referred to as *Grasp*$^{-/-}$ hereafter). Immunoblot analysis from brain extracts confirmed the loss of Grasp protein expression in *Grasp*$^{-/-}$ mice (Fig. 1E, lower panel). Under basal conditions, *Grasp*$^{-/-}$ mice showed no morphological, behavioral or sexual defects (data not shown), as previously reported by others[7].

An acute dose of UVB leads to induction of *Grasp* in skin

Unlike ATRA treatment of P19 embryonal carcinoma cells[1], topical application of ATRA did not induce expression of *Grasp* transcripts in mouse skin (unpublished data). *Grasp* expression was predominantly restricted to the epidermal layers of skin, including the hair shaft, under basal conditions (Fig. 2A). However, a single UVB exposure resulted in a ~13-fold up-regulation of *Grasp* transcripts in wt mouse skin (Fig. 2B, E). A striking induction of *Grasp* transcripts was observed primarily in the dermal layers of wt skin, and to a lesser extent in the epidermis, following UVB exposure (compare Figs. 2A and 2B). *Grasp* transcripts were not detected in tissues from *Grasp*$^{-/-}$ mice (Figs. 2C, D). UVB-induced expression of *Grasp* was recapitulated in primary dermal fibroblasts from wt mice (Fig. 2F), in which a single exposure to UVB irradiation resulted in a ~125 fold induction of *Grasp* expression within 6 hrs that was still evident at 24 hrs after exposure (Fig. 2F). UVB-induced expression of Grasp was not detected in cultured, primary keratinocytes from wild-type mice (Fig. S2).

Delayed epidermal thickening in *Grasp*$^{-/-}$ mice following acute exposure to UVB irradiation

Epidermal hyperplasia, the hallmark response of UVB exposure, occurs within 24 hrs of exposure[14]. To evaluate the role of *Grasp* in UV-induced epidermal hyperplasia, wt and *Grasp*$^{-/-}$ mice were subjected to acute UVB irradiation and analysed for morphological changes, and alterations in cellular proliferation and differentiation. Histological analysis by H&E staining revealed a significant increase in the epidermal thickness of skin in wt mice after 24 hrs (compare Figs. 3A and 3B). Epidermal thickness returned to basal levels in wt mice 48 hrs after acute UVB exposure (compare Figs. 3A and 3C). The rapid return of the hyperplasia response to basal state within 48 hours of UVB exposure in the littermate controls contrasts with the persistent hyperplasia response observed in purebred C57BL/6 mice[31–33]. This observation is indicative of the high UVB resistance of the background strain of the *Grasp*$^{-/-}$ littermate controls. In contrast, *Grasp*$^{-/-}$ mice exhibited no obvious change in epidermal thickness 24 hrs post-UV (compare Figs. 3D and 3E), but a delayed epidermal hyperplasia was evident at 48 hrs after UVB exposure in mutant skin (compare Figs. 3D and 3F). Although the epidermal response to UVB exposure was delayed in *Grasp*$^{-/-}$ mice, hyperplasia in the mutants was 2.4-fold greater than that of wt mice at 48 hrs after a single UVB exposure (2-way ANOVA, Interaction, $F_{(2,174)} = 17.58$, $p < 0.0001$; effect of time, $F_{(2,174)} = 21.07$, $p < 0.0001$; effect of genotype, $F_{(1,174)}=0.7741$, $p=0.3802$; Fig 3G). These results indicate an important role of *Grasp* in maintaining epidermal homeostasis after an acute dose of UVB irradiation. It is conceivable that enhanced proliferative capacity or lack of induced apoptosis may underlie, at least in part, epidermal thickening observed in *Grasp*$^{-/-}$ mice at 48 hrs following UVB exposure.

Grasp$^{-/-}$ mice display altered proliferative response to UVB treatment

We hypothesized that the delay in epidermal response after UVB exposure was due to a delayed proliferative response in *Grasp*$^{-/-}$ mice. We compared the proliferative index of *Grasp*$^{-/-}$ and wt mice skin by ratioing $BrdU^+$ cells to $DAPI^+$ nuclei in the basal ($K14^+$) cell layer of the epidermis before and after UVB exposure. Under basal conditions, we observed no significant difference in the percentages of $BrdU^+$ epidermal cells in *Grasp*$^{-/-}$ mice and wt controls (compare Figs. 4A and B; see also Fig. 4G). Following UVB treatment, basal cells of the inter-follicular epithelium are known to enter S-phase rapidly and proliferate[34, 35]. The majority of $BrdU^+$ cells in skin samples obtained at 24 hrs post-UVB exposure corresponded to slow-cycling cells of the intrafollicular epidermis in both mutant and wt mice (Fig. 4C, D, and G). A significant increase in detectable levels of $BrdU^+$ cells was observed in inter- and intra-follicular epidermis of both wt and mutant mice after 48 hrs of UV exposure (Fig. 4E and F). However, the number of $BrdU^+$ epidermal cells observed in *Grasp*$^{-/-}$ mice was significantly lower compared to wt littermates at 48 hrs post-UV exposure (2-way ANOVA, Interaction, $F_{(2,138)} = 10.27$, $p < 0.0001$; effect of time, $F_{(2,138)} = 44.72$, $p < 0.0001$; effect of genotype, $F_{(1,138)} = 11.52$, $p < 0.0001$; Fig 4G). When compared to wt, anti-K14 immunoreactivity was lower in *Grasp*$^{-/-}$ skin at 24 hrs post-UVB exposure (compare panels C and D of Fig. 4 and panels B and D of Fig. S3). However, expression of other markers of epidermal differentiation, including keratin K10, loricrin, and filaggrin

were unaffected in *Grasp*$^{-/-}$ mice as compared to wt skin (see Fig. S3). These results suggest that *Grasp*$^{-/-}$ mice exhibit a reduced proliferative response to UVB exposure.

Dysregulated apoptotic responses are observed in *Grasp*$^{-/-}$ mice following UVB exposure

Our data suggest that Grasp may regulate UVB-induced apoptosis in skin and a dysregulated apoptotic response may underlie the observed phenotype of *Grasp*$^{-/-}$ mice following UVB exposure. A robust apoptotic signal, detected by TUNEL staining, was observed in wt skin at 24 and 48 hrs after UVB treatment (Figs. 5C and 5E, respectively). However, the apoptotic signal was almost completely absent in *Grasp*$^{-/-}$ skin examined at 48 hrs post-UV treatment (compare Figs. 5E and 5F). Taken together our results suggest an important role of *Grasp* in mediating apoptotic responses in skin after UVB exposure

Reduced nuclear accumulation of p53 in epidermal cells of *Grasp*$^{-/-}$ mice after UVB treatment

Altered proliferative and apoptotic responses in *Grasp*$^{-/-}$ mice may be due to dysregulation at one or more levels of the p53 signaling pathway. We carried out RT-qPCR analysis to assess *p53* transcript levels in wt and *Grasp*$^{-/-}$ mice skin. In accordance with published reports (25), we found that UVB exposure did not alter *p53* transcript levels in wt mice, and this finding generalized to *Grasp*$^{-/-}$ mice (Fig. S4A). However, wt and *Grasp*$^{-/-}$ littermates exhibited a robust and sustained increase in the levels of p53 protein at 24 and 48 hrs post-UV treatments (Fig. S4B).

Standard immunohistochemical analyses were performed on skin samples using the CM5-p53 antibody, in order to determine if sub-cellular localization of p53 was altered in *Grasp*$^{-/-}$ mice in response to UVB treatment. Nuclear localization of the p53 was validated by co-localization with the nuclear counterstain DAPI and the transcription factor Ctip2/Bcl11b, which is highly expressed in basal layers of the skin[27] (Fig. 4 and data not shown). We observed a robust increase in nuclear localization of p53 after 24 hrs of UVB treatment in wt (30.3 ± 2.9% of the epidermal cells, compare Figs. 4A and 4C) and the proportion of cells exhibiting p53 staining in the nucleus was maintained to at least 48 hrs post-UVB exposure (25.1 ± 2.1% of the epidermal cells; compare Figs. 4A and 4E). Although we observed a similar increase in nuclear p53 staining after UVB exposure in *Grasp*$^{-/-}$ mice, the relative levels of nuclear p53 were significantly lower in *Grasp*$^{-/-}$ mice as compared to wt mice (2-way ANOVA, Interaction, $F_{(2,137)} = 10.36$, $p < 0.0001$; effect of time, $F_{(2,137)} = 111.2$, $p < 0.0001$; effect of genotype, $F_{(1,137)} = 24.63$, $p < 0.0001$). At 24hrs post-UV, post-hoc test reveal that the reduced levels of p53^{+} epidermal cells in *Grasp*$^{-/-}$ mice tended towards statistical significance (Bonferroni's multiple comparisons test. $p = 0.0622$, wt = 29.7 ± 3.3%, *Grasp*$^{-/-}$ = 24.6 ± 1.1% of epidermal cells) and became more pronounced after 48 hrs post-UV exposure (Bonferroni's multiple comparisons test. $p < 0.0001$, wt = 25.1 ± 2.1%, *Grasp*$^{-/-}$ = 9.0 ± 1.8% of epidermal cells). Taken together, our results confirm that *Grasp*$^{-/-}$ mice exhibit only a transient increase in nuclear localization of p53 protein in response to UVB treatment, suggesting a potential role of Grasp in post-translational modification and/or sub-cellular localization of the tumor suppressor protein p53.

Discussion

In the present study we report the generation of *Grasp*$^{-/-}$ mice with a germline disruption of the *Grasp* gene. Lack of Grasp expression clearly impacted the response of the skin to a single dose of UVB irradiation, resulting in delayed proliferative and dampened apoptotic responses. These findings suggest that Grasp may play a role in the skin's response to acute UVB exposure, which is causally implicated in melanoma and non-melanocytic skin cancer[36–40]. Grasp is abundantly expressed in neuronal tissue[1–3] and functions in protein trafficking[2, 4–6], neuroplasticity[8], and perhaps in behavioural responses to cocaine and morphine[7]. However, understanding the *in vivo* role of *Grasp* has been hindered by the relative inaccessibility and complexity of nervous tissue as a model system.

Skin provides an excellent alternative with its accessibility and simplicity, and a well-characterized, robust response to physical and chemical insults[10–17]. Unlike ATRA treatment in P19 embryonal carcinoma cells[1], topical application of ATRA did not induce *Grasp* transcripts in mouse skin (unpublished data). Expression of *Grasp* was robustly induced after a single dose of UVB, and this induction was particularly noteworthy in the dermal compartment of skin (see Fig. 2). Our understanding of dermal responses to UVB exposure has largely been limited to: (i) a hyper-vascularization response accompanied with a large increase in infiltrating macrophages, neutrophils, and Langerhans cells, and a cascade of events that lead to suppression of the innate immunity of skin[33, 41–46], and (ii) a poorly understood signaling cascade in dermal fibroblasts that causes major alterations in the dermal extracellular matrix owing to activation of metalloproteinases[47–49]. As *Grasp* is poorly expressed in the immune system (our unpublished data), our data suggest that Grasp may play a role in the latter process. Future efforts will investigate the status of dermal elastin and collagen following UVB exposure in *Grasp*$^{-/-}$ mice, which could provide new insights relevant to photo-damage and aging. UVB-induced expression of *Grasp* was not evident in cultured, primary keratinocytes, which indicates that regulation of Grasp expression by UVB may be a cell-type specific event, require a non-cell autonomous factor(s), and/or be dependent on the complex, three-dimensional microenvironment of intact skin.

Our observations in the present study indicate reduced proliferative and apoptotic responses to UVB exposure in skin of mice lacking Grasp. Although not reaching statistical significance, *Grasp*$^{-/-}$ mice displayed a thicker epidermis (30% thicker; $p > 0.05$) relative to wt littermates, even under basal conditions (Fig. 3G; 1.05 ± 0.05 mm and 1.37 ± 0.05 mm for wt and mutant epidermis, respectively). This increase in epidermal thickness was observed despite the fact that the proliferative index of *Grasp*$^{-/-}$ epidermis was lower than that of wt mice both before and after UVB exposure (Fig. 4G). This finding strongly suggests that reduced apoptosis in *Grasp*$^{-/-}$ epidermis is the predominant driver of epidermal hyperplasia observed in the mice lacking Grasp.

Dysregulated apoptosis and/or uncontrolled proliferation of cells observed following acute UVB damage are often attributed to a disruption of the complex, regulatory processes of p53 induction, stabilization, and/or sub-cellular localization[14, 16, 19, 21, 50–57]. Our data suggest that steady-state levels of the *p53* transcript and the induction of p53 protein following UVB

exposure are comparable in wt mice and *Grasp*$^{-/-}$ littermates (see Figs. S2A, B). However, *Grasp*$^{-/-}$ mice exhibit a significant attenuation in nuclear accumulation of p53 following UVB treatment, indicative of dysregulated nuclear import and/or export of the p53 protein. The loss of p53 from the nuclear compartment coincided precisely with loss of TUNEL^{+} cells in the epidermis (see Fig. 4), strongly suggesting that the altered response following UVB exposure in *Grasp*$^{-/-}$ mice was due to dysregulation of the p53-regulated apoptotic pathway. An inferential extension of an attenuated apoptotic response is that *Grasp*$^{-/-}$ mice will be more susceptible to UVB induced photocarcinogenesis. This will be working hypothesis for future studies.

Another prediction of the transient nuclear accumulation of p53 would be a loss in the p53-dependent G1/S arrest of cell-cycle [58–60], which should lead to increased rate of DNA synthesis and progression in the S-phase of cell-cycle. However, we observe reduced levels of BrdU incorporation within the epidermal cells of *Grasp*$^{-/-}$ mice when compared to littermate controls at 48 hours post-UVB exposure (see Fig. 4G). This would indicate either an unchanged or reduced rate of DNA synthesis in the epidermal cell cycle of *Grasp*$^{-/-}$ mice. This paradox can potentially be attributed to the role of p53-indendepent pathways that have been increasingly implicated in regulating cell-cycle checkpoints[61], particularly after UV radiation[62, 63]. To summarize, *Grasp*$^{-/-}$ mice exhibit a complex and distinct dysregulation of homeostatic responses following UVB exposure.

Conclusions

Our results indicate a potential role of Grasp in the p53-mediated response of skin to UVB exposure. The underlying importance of this study is highlighted by the finding that over 50% of all known cancers have been linked to dysregulation in one or more of the many p53-dependent pathways[20, 21]. Future research will further our understanding of the mechanism(s) of Grasp-mediated nuclear transport/stabilization of p53. This study indicates that Grasp likely plays a minimal role in embryological development or basal homeostasis in post-natal and adult mice. However, under conditions of induced stress, such as UVB exposure or morphine administration[7], the *in vivo* role of *Grasp* was revealed. Our findings indicate a potential role of *Grasp* as “late gene,” in that *Grasp* was up-regulated following an imbalance in the dynamic equilibrium of skin. It will therefore be necessary to assess the role of *Grasp* in other proliferative paradigms in the skin (and/or other model systems) to further our understanding of the *in vivo* role of this important protein.

Supplementary Material

Refer to Web version on PubMed Central for supplementary material.

Acknowledgments

This work was supported by grants ES00040 and ES000210 from the National Institute of Environmental Health Sciences to the Environmental Health Sciences Center at Oregon State University.

References

1. Nevrivy DJ, Peterson VJ, Avram D, Ishmael JE, Hansen SG, Dowell P, Hruby DE, Dawson MI, Leid M. Interaction of GRASP, a protein encoded by a novel retinoic acid-induced gene, with members of the cytohesin family of guanine nucleotide exchange factors. J Biol Chem. 2000; 275:16827–16836. [PubMed: 10828067]
2. Kitano J, Kimura K, Yamazaki Y, Soda T, Shigemoto R, Nakajima Y, Nakanishi S. Tamalin, a PDZ domain-containing protein, links a protein complex formation of group 1 metabotropic glutamate receptors and the guanine nucleotide exchange factor cytohesins. J Neurosci. 2002; 22:1280–1289. [PubMed: 11850456]
3. Kitano J, Yamazaki Y, Kimura K, Masukado T, Nakajima Y, Nakanishi S. Tamalin is a scaffold protein that interacts with multiple neuronal proteins in distinct modes of protein-protein association. J Biol Chem. 2003; 278:14762–14768. [PubMed: 12586822]
4. Esteban PF, Yoon HY, Becker J, Dorsey SG, Caprari P, Palko ME, Coppola V, Saragovi HU, Randazzo PA, Tessarollo L. A kinase-deficient TrkC receptor isoform activates Arf6-Rac1 signaling through the scaffold protein tamalin. J Cell Biol. 2006; 173:291–299. [PubMed: 16636148]
5. Sugi T, Oyama T, Muto T, Nakanishi S, Morikawa K, Jingami H. Crystal structures of autoinhibitory PDZ domain of Tamalin: implications for metabotropic glutamate receptor trafficking regulation. EMBO J. 2007; 26:2192–2205. [PubMed: 17396155]
6. Venkataraman A, Nevrivy DJ, Filtz TM, Leid M. Grp1-associated scaffold protein (GRASP) is a regulator of the ADP ribosylation factor 6 (Arf6)-dependent membrane trafficking pathway. Cell biology international. 2012; 36:1115–1128. [PubMed: 22931251]
7. Ogawa M, Miyakawa T, Nakamura K, Kitano J, Furushima K, Kiyonari H, Nakayama R, Nakao K, Moriyoshi K, Nakanishi S. Altered sensitivities to morphine and cocaine in scaffold protein tamalin knockout mice. Proc Natl Acad Sci U S A. 2007; 104:14789–14794. [PubMed: 17766434]
8. Yanpallewar SU, Barrick CA, Palko ME, Fulgenzi G, Tessarollo L. Tamalin is a critical mediator of electroconvulsive shock-induced adult neuroplasticity. J Neurosci. 2012; 32:2252–2262. [PubMed: 22396401]
9. Mo J, Choi S, Ahn PG, Sun W, Lee HW, Kim H. PDZ-scaffold protein, Tamalin promotes dendritic outgrowth and arborization in rat hippocampal neuron. Biochemical and biophysical research communications. 2012; 422:250–255. [PubMed: 22569042]
10. Fisher GJ, Voorhees JJ. Molecular mechanisms of retinoid actions in skin. FASEB J. 1996; 10:1002–1013. [PubMed: 8801161]
11. Chapellier B, Mark M, Messaddeq N, Calleja C, Warot X, Brocard J, Gerard C, Li M, Metzger D, Ghyselinck NB, Chambon P. Physiological and retinoid-induced proliferations of epidermis basal keratinocytes are differently controlled. EMBO J. 2002; 21:3402–3413. [PubMed: 12093741]
12. Abel EL, Angel JM, Kiguchi K, DiGiovanni J. Multi-stage chemical carcinogenesis in mouse skin: fundamentals and applications. Nat Protoc. 2009; 4:1350–1362. [PubMed: 19713956]
13. Lee JK, Kim JH, Nam KT, Lee SH. Molecular events associated with apoptosis and proliferation induced by ultraviolet-B radiation in the skin of hairless mice. J Dermatol Sci. 2003; 32:171–179. [PubMed: 14507442]
14. Ouhtit A, Muller HK, Davis DW, Ullrich SE, McConkey D, Ananthaswamy HN. Temporal events in skin injury and the early adaptive responses in ultraviolet-irradiated mouse skin. Am J Pathol. 2000; 156:201–207. [PubMed: 10623668]
15. Ouhtit A, Ananthaswamy HN. A Model for UV-Induction of Skin Cancer. J Biomed Biotechnol. 2001; 1:5–6. [PubMed: 12488619]
16. Matsumura Y, Ananthaswamy HN. Short-term and long-term cellular and molecular events following UV irradiation of skin: implications for molecular medicine. Expert Rev Mol Med. 2002; 4:1–22. [PubMed: 14585163]
17. Melnikova VO, Ananthaswamy HN. Cellular and molecular events leading to the development of skin cancer. Mutat Res. 2005; 571:91–106. [PubMed: 15748641]
18. Fuchs E. Scratching the surface of skin development. Nature. 2007; 445:834–842. [PubMed: 17314969]

19. Lippens S, Hoste E, Vandenabeele P, Agostinis P, Declercq W. Cell death in the skin. Apoptosis. 2009; 14:549–569. [PubMed: 19221876]
20. Strano S, Dell'Orso S, Di Agostino S, Fontemaggi G, Sacchi A, Blandino G. Mutant p53: an oncogenic transcription factor. Oncogene. 2007; 26:2212–2219. [PubMed: 17401430]
21. Murray-Zmijewski F, Slee EA, Lu X. A complex barcode underlies the heterogeneous response of p53 to stress. Nat Rev Mol Cell Biol. 2008; 9:702–712. [PubMed: 18719709]
22. Kawabe TT, Kubicek MF, Johnson GA, Buhl AE. Use of gamma-glutamyl transpeptidase activity as a marker of hair cycle and anagen induction in mouse hair follicles. The Journal of investigative dermatology. 1994; 103:122–126. [PubMed: 7913117]
23. Stenn KS, Paus R. Controls of hair follicle cycling. Physiol Rev. 2001; 81:449–494. [PubMed: 11152763]
24. Silver, A.; HBC; Arsenault, C. Early anagen initiated by plucking compared with early spontaneous anagen. Pergamon Press; London, UK: 1967.
25. Wang Z, Coleman DJ, Bajaj G, Liang X, Ganguli-Indra G, Indra AK. RXRalpha ablation in epidermal keratinocytes enhances UVR-induced DNA damage, apoptosis, and proliferation of keratinocytes and melanocytes. The Journal of investigative dermatology. 131:177–187. [PubMed: 20944655]
26. Indra AK, Dupe V, Bornert JM, Messaddeq N, Yaniv M, Mark M, Chambon P, Metzger D. Temporally controlled targeted somatic mutagenesis in embryonic surface ectoderm and fetal epidermal keratinocytes unveils two distinct developmental functions of BRG1 in limb morphogenesis and skin barrier formation. Development. 2005; 132:4533–4544. [PubMed: 16192310]
27. Golonzhka O, Leid M, Indra G, Indra AK. Expression of COUP-TF-interacting protein 2 (CTIP2) in mouse skin during development and in adulthood. Gene Expr Patterns. 2007; 7:754–760. [PubMed: 17631058]
28. Bookout AL, Mangelsdorf DJ. Quantitative real-time PCR protocol for analysis of nuclear receptor signaling pathways. Nucl Recept Signal. 2003; 1:e012. [PubMed: 16604184]
29. Rodriguez CI, Buchholz F, Galloway J, Sequerra R, Kasper J, Ayala R, Stewart AF, Dymecki SM. High-efficiency deleter mice show that FLPe is an alternative to Cre-loxP. Nat Genet. 2000; 25:139–140. [PubMed: 10835623]
30. O'Gorman S, Dagenais NA, Qian M, Marchuk Y. Protamine-Cre recombinase transgenes efficiently recombine target sequences in the male germ line of mice, but not in embryonic stem cells. Proc Natl Acad Sci U S A. 1997; 94:14602–14607. [PubMed: 9405659]
31. Hanada K, Sawamura D, Hashimoto I, Kida K, Naganuma A. Epidermal proliferation of the skin in metallothionein-null mice. The Journal of investigative dermatology. 1998; 110:259–262. [PubMed: 9506445]
32. Kurimoto I, Streilein JW. Characterization of the immunogenetic basis of ultraviolet-B light effects on contact hypersensitivity induction. Immunology. 1994; 81:352–358. [PubMed: 8206509]
33. Clydesdale GJ, Dandie GW, Muller HK. Ultraviolet light induced injury: immunological and inflammatory effects. Immunol Cell Biol. 2001; 79:547–568. [PubMed: 11903614]
34. de Laat A, Kroon ED, de Gruijl FR. Cell cycle effects and concomitant p53 expression in hairless murine skin after longwave UVA (365 nm) irradiation: a comparison with UVB irradiation. Photochem Photobiol. 1997; 65:730–735. [PubMed: 9114751]
35. Rebel HG, Bodmann CA, van de Glind GC, de Gruijl FR. UV-induced ablation of the epidermal basal layer including p53-mutant clones resets UV carcinogenesis showing squamous cell carcinomas to originate from interfollicular epidermis. Carcinogenesis. 33:714–720. [PubMed: 22227037]
36. Mottram PL, Mirisklavos A, Clunie GJ, Noonan FP. A single dose of UV radiation suppresses delayed type hypersensitivity responses to alloantigens and prolongs heart allograft survival in mice. Immunol Cell Biol. 1988; 66(Pt 5–6):377–385. [PubMed: 2976024]
37. Noonan F, De Fabo EC. UV immunosuppression and skin cancer. J Invest Dermatol. 1998; 111:706–708. [PubMed: 9764859]
38. Noonan FP, Recio JA, Takayama H, Duray P, Anver MR, Rush WL, De Fabo EC, Merlino G. Neonatal sunburn and melanoma in mice. Nature. 2001; 413:271–272. [PubMed: 11565020]

39. Noonan FP, Muller HK, Fears TR, Kusewitt DF, Johnson TM, De Fabo EC. Mice with genetically determined high susceptibility to ultraviolet (UV)-induced immunosuppression show enhanced UV carcinogenesis. J Invest Dermatol. 2003; 121:1175–1181. [PubMed: 14708623]
40. Wang Z, Coleman DJ, Bajaj G, Liang X, Ganguli-Indra G, Indra AK. RXRalpha ablation in epidermal keratinocytes enhances UVR-induced DNA damage, apoptosis, and proliferation of keratinocytes and melanocytes. J Invest Dermatol. 2011; 131:177–187. [PubMed: 20944655]
41. Yano K, Kajiya K, Ishiwata M, Hong YK, Miyakawa T, Detmar M. Ultraviolet B-induced skin angiogenesis is associated with a switch in the balance of vascular endothelial growth factor and thrombospondin-1 expression. J Invest Dermatol. 2004; 122:201–208. [PubMed: 14962109]
42. Hamakawa M, Sugihara A, Okamoto H, Horio T. Ultraviolet B radiation suppresses Langerhans cell migration in the dermis by down-regulation of alpha4 integrin. Photodermatol Photoimmunol Photomed. 2006; 22:116–123. [PubMed: 16719863]
43. Meunier L. Ultraviolet light and dendritic cells. Eur J Dermatol. 1999; 9:269–275. [PubMed: 10356402]
44. Piskin G, Bos JD, Teunissen MB. Neutrophils infiltrating ultraviolet B-irradiated normal human skin display high IL-10 expression. Arch Dermatol Res. 2005; 296:339–342. [PubMed: 15551142]
45. Aubin F. Mechanisms involved in ultraviolet light-induced immunosuppression. Eur J Dermatol. 2003; 13:515–523. [PubMed: 14721768]
46. Rijken F, Kiekens RC, van den Worm E, Lee PL, van Weelden H, Bruijnzeel PL. Pathophysiology of photoaging of human skin: focus on neutrophils. Photochem Photobiol Sci. 2006; 5:184–189. [PubMed: 16465304]
47. Brenneisen P, Sies H, Scharffetter-Kochanek K. Ultraviolet-B irradiation and matrix metalloproteinases: from induction via signaling to initial events. Ann N Y Acad Sci. 2002; 973:31–43. [PubMed: 12485830]
48. Oh JH, Kim A, Park JM, Kim SH, Chung AS. Ultraviolet B-induced matrix metalloproteinase-1 and −3 secretions are mediated via PTEN/Akt pathway in human dermal fibroblasts. J Cell Physiol. 2006; 209:775–785. [PubMed: 16972255]
49. Dong KK, Damaghi N, Picart SD, Markova NG, Obayashi K, Okano Y, Masaki H, Grether-Beck S, Krutmann J, Smiles KA, Yarosh DB. UV-induced DNA damage initiates release of MMP-1 in human skin. Exp Dermatol. 2008; 17:1037–1044. [PubMed: 18459971]
50. Halaby MJ, Yang DQ. p53 translational control: a new facet of p53 regulation and its implication for tumorigenesis and cancer therapeutics. Gene. 2007; 395:1–7. [PubMed: 17395405]
51. Mazan-Mamczarz K, Galban S, Lopez de Silanes I, Martindale JL, Atasoy U, Keene JD, Gorospe M. RNA-binding protein HuR enhances p53 translation in response to ultraviolet light irradiation. Proc Natl Acad Sci U S A. 2003; 100:8354–8359. [PubMed: 12821781]
52. Olsson A, Manzl C, Strasser A, Villunger A. How important are post-translational modifications in p53 for selectivity in target-gene transcription and tumour suppression? Cell Death Differ. 2007; 14:1561–1575. [PubMed: 17627286]
53. Lavin MF, Gueven N. The complexity of p53 stabilization and activation. Cell Death Differ. 2006; 13:941–950. [PubMed: 16601750]
54. Giannakakou P, Nakano M, Nicolaou KC, O'Brate A, Yu J, Blagosklonny MV, Greber UF, Fojo T. Enhanced microtubule-dependent trafficking and p53 nuclear accumulation by suppression of microtubule dynamics. Proc Natl Acad Sci U S A. 2002; 99:10855–10860. [PubMed: 12145320]
55. Jackson MW, Patt LE, LaRusch GA, Donner DB, Stark GR, Mayo LD. Hdm2 nuclear export, regulated by insulin-like growth factor-I/MAPK/p90Rsk signaling, mediates the transformation of human cells. J Biol Chem. 2006; 281:16814–16820. [PubMed: 16621805]
56. O'Brate A, Giannakakou P. The importance of p53 location: nuclear or cytoplasmic zip code? Drug Resist Updat. 2003; 6:313–322. [PubMed: 14744495]
57. Inoue T, Wu L, Stuart J, Maki CG. Control of p53 nuclear accumulation in stressed cells. FEBS Lett. 2005; 579:4978–4984. [PubMed: 16115632]
58. Bartek J, Lukas J. Mammalian G1- and S-phase checkpoints in response to DNA damage. Curr Opin Cell Biol. 2001; 13:738–747. [PubMed: 11698191]
59. Sengupta S, Harris CC. p53: traffic cop at the crossroads of DNA repair and recombination. Nat Rev Mol Cell Biol. 2005; 6:44–55. [PubMed: 15688066]

60. Agarwal ML, Agarwal A, Taylor WR, Stark GR. p53 controls both the G2/M and the G1 cell cycle checkpoints and mediates reversible growth arrest in human fibroblasts. Proc Natl Acad Sci U S A. 1995; 92:8493–8497. [PubMed: 7667317]

61. Sherr CJ. Divorcing ARF and p53: an unsettled case. Nat Rev Cancer. 2006; 6:663–673. [PubMed: 16915296]

62. Al-Mohanna MA, Al-Khodairy FM, Krezolek Z, Bertilsson PA, Al-Houssein KA, Aboussekhra A. p53 is dispensable for UV-induced cell cycle arrest at late G(1) in mammalian cells. Carcinogenesis. 2001; 22:573–578. [PubMed: 11285191]

63. Loignon M, Drobetsky EA. The initiation of UV-induced G(1) arrest in human cells is independent of the p53/p21/pRb pathway but can be attenuated through expression of the HPV E7 oncoprotein. Carcinogenesis. 2002; 23:35–45. [PubMed: 11756221]

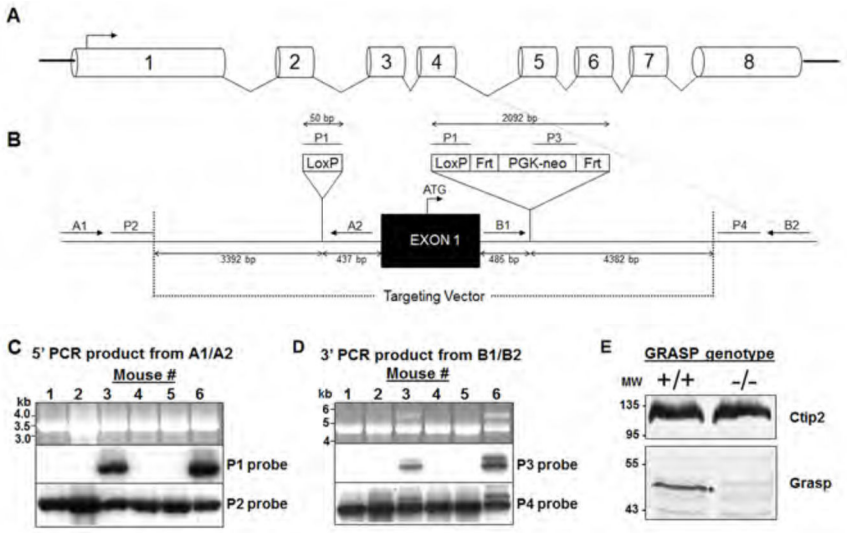

Fig. 1.

Generation of mice harboring a germline disruption of the *Grasp* locus (*Grasp*$^{-/-}$). (A) Schematic representation of the genomic organization of the eight exons of the mouse *Grasp* locus. (B) The *Grasp* targeting vector indicating the upstream and downstream LoxP sites and the PGK-Neo cassette, the latter of which was flanked by Frt sites. (C–D) Southern analysis of homologous recombination (HR) at the *Grasp* locus using long-template PCR (see Table S1 for sequences of primers and probes). (C) The amplification product at the 5′ end (primers A1/A2) was probed with P1 and P2 (inside and outside respectively of the targeting vector) to identify the clones in which HR had occurred. (D) The 3′ PCR product (primers A3/A4) was also probed with P3 and P4 (inside and outside respectively, of the targeting vector to identify the HR^{+} clones. The doublet observed in lanes 3 and 6 corresponds to the absence (wt) and presence (L3) of the LoxP-Frt-PGK neo-Frt cassette. No such doublet was observed in lanes 3 and 6 of (C) because of the small size of the insertion at the 5′ loxP site. (E) Immunoblot analysis of whole brain extracts prepared from wt and *Grasp*$^{-/-}$ mice using anti-Grasp and anti-Bcl11b (loading control) antibodies. The band corresponding to Grasp is denoted by an asterisk.

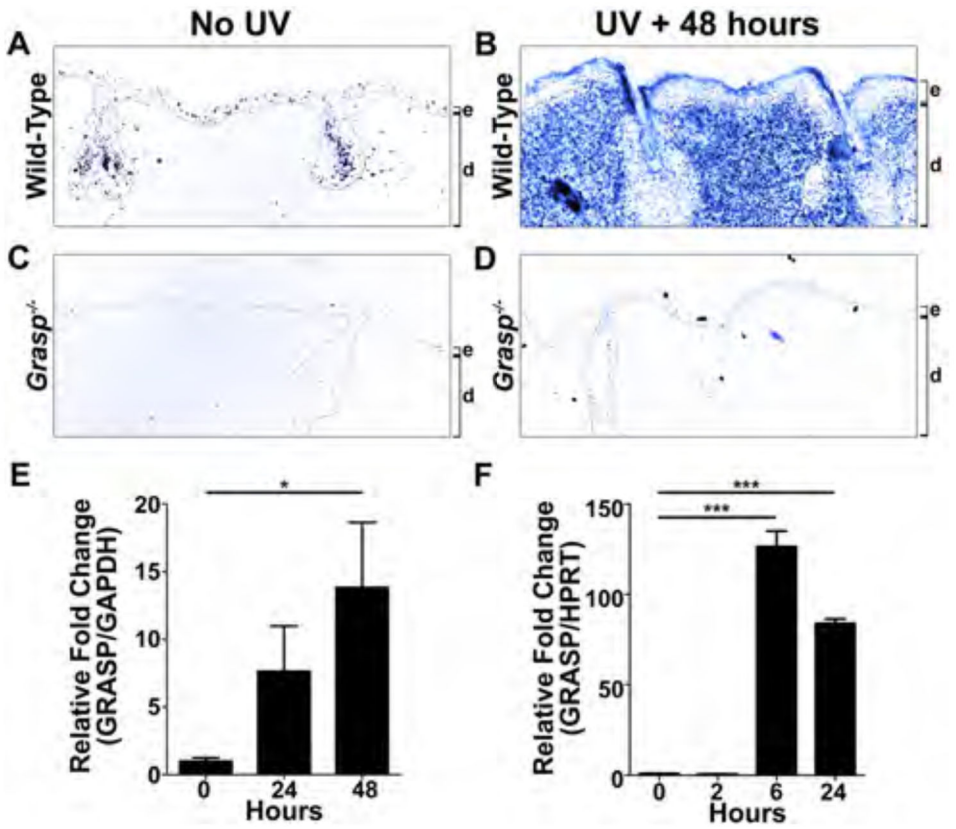

Fig. 2.

Grasp is induced in the epidermal and dermal layers of skin following a single UVB exposure. (A–D) In situ hybridization of skin samples using a *Grasp* cRNA probe. Skin samples were collected from wild-type or *Grasp*$^{-/-}$ mice at indicated times after UVB exposure. (E) RT-qPCR analysis of *Grasp* transcripts in skin samples prepared from wt mice at indicated times after UVB exposure. (F) RT-qPCR analysis of *Grasp* transcripts in cultured skin fibroblasts prepared from wt mice and collected at indicated times after UVB exposure. Values in (E,F) and represent the mean ± S.E.M. of three independent mice and cell-culture experiments respectively for each time point. Statistical significance is indicated by * and *** symbols for $p < 0.05$ and $p < 0.001$, respectively.

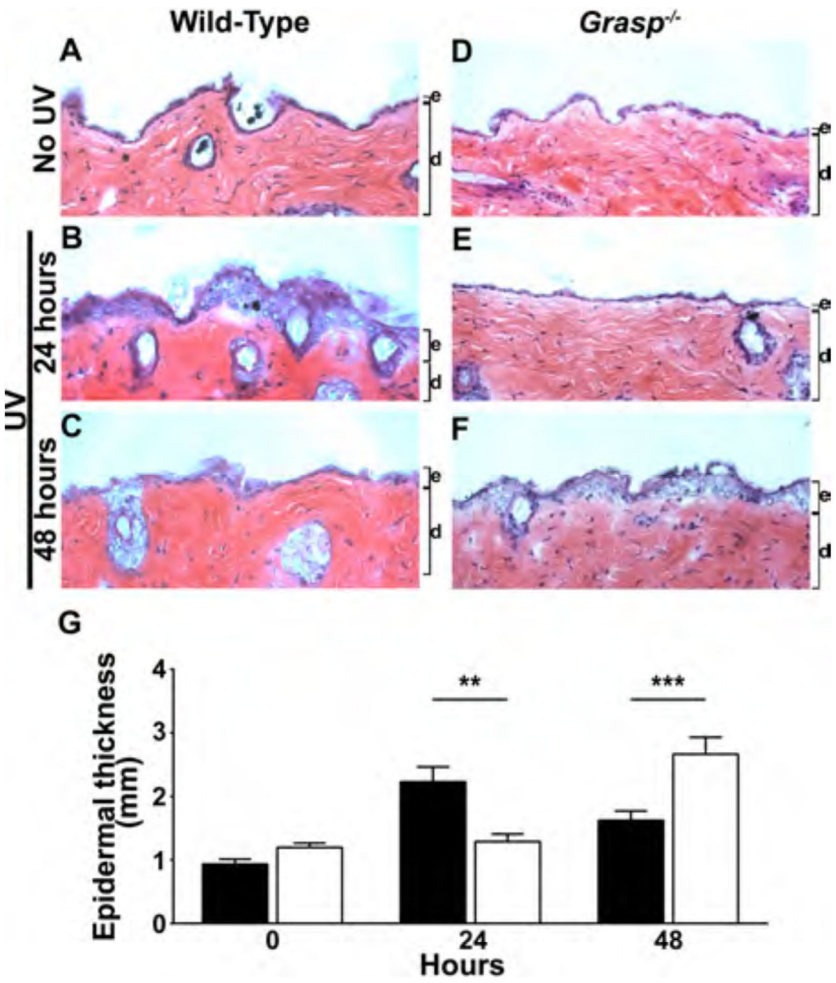

Fig. 3.

Grasp$^{-/-}$ mice exhibit delayed epidermal thickening in response to UVB exposure. (A–F) H&E-stained histological sections obtained at indicated time intervals after UVB exposure from wild type (A–C) and *Grasp*$^{-/-}$ mice (D–F). Scale bar, 50 μM. (G) Quantitation of epidermal thickness at indicated times intervals following UVB exposure. Values in (G) represent the mean ± S.E.M. of three mice for each time point and genotype. Statistical significance and is indicated by ** and *** symbols for $p < 0.001$ and $p < 0.0001$, respectively.

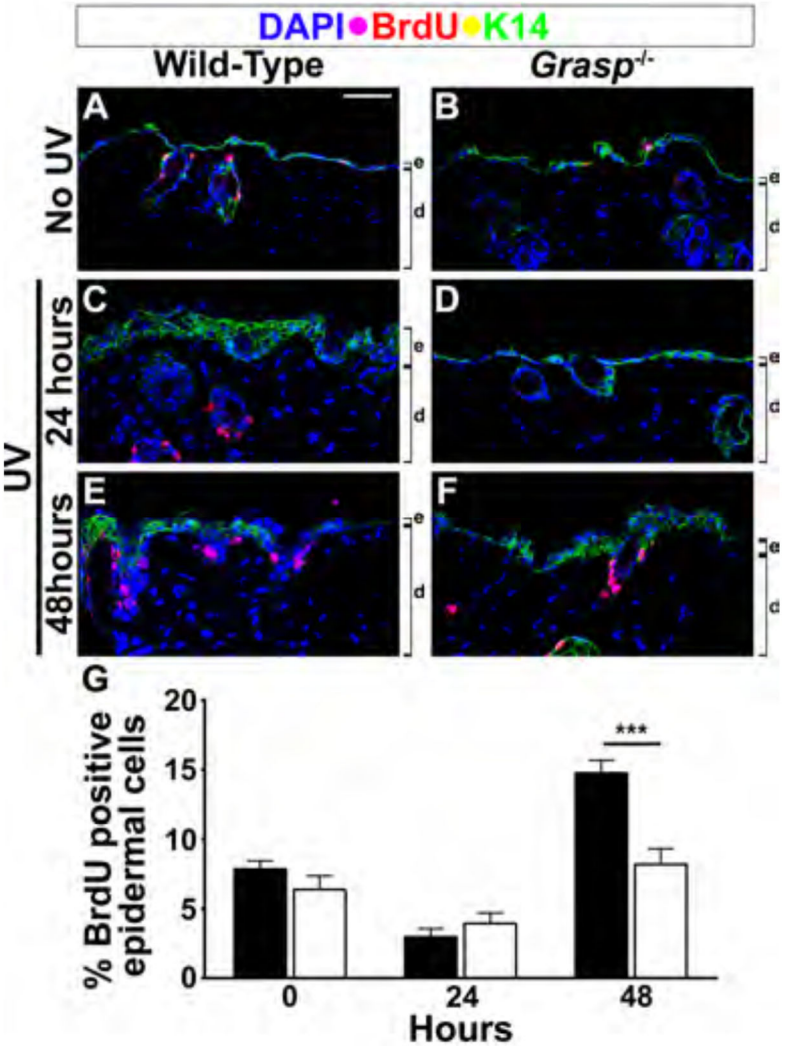

Fig. 4.

Grasp$^{-/-}$ mice exhibit a reduced proliferative response to UVB exposure. (A–F) BrdU (red) and K14 (green) immunohistochemical staining in skin samples obtained at indicated time intervals after UVB exposure. Scale bar, 50 μM. (G) Quantitation of BrdU^{+}/K14^{+} cells of the epidermis at indicated time intervals following UVB exposure. Values in (G) represent the mean ± S.E.M. of three *Grasp*$^{-/-}$ mice and littermate controls for each time point. Statistical significance is indicated by *** for $p < 0.0001$.

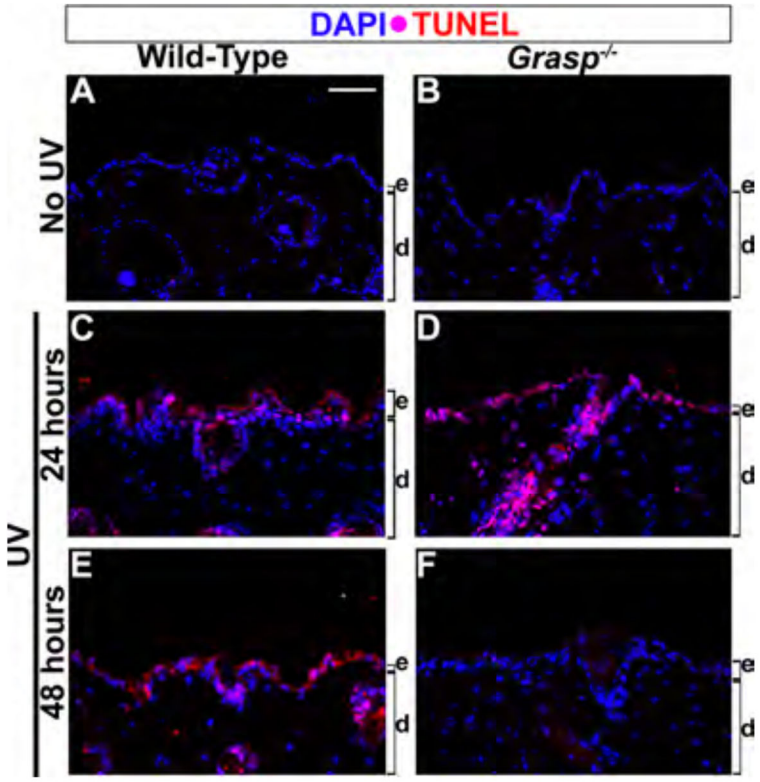

Fig. 5.

Grasp$^{-/-}$ mice exhibit attenuated apoptotic response to UVB exposure. (A–F) The TUNEL assay shown was performed in wt and mutant skin at indicated time intervals after UVB exposure. Skin samples were counterstained with the nuclear stain DAPI. Scale bars = 50 μM. Sections from individual mice are shown in A–F. These mice are representative of four to seven mice of each genotype that were analyzed at each time point indicated

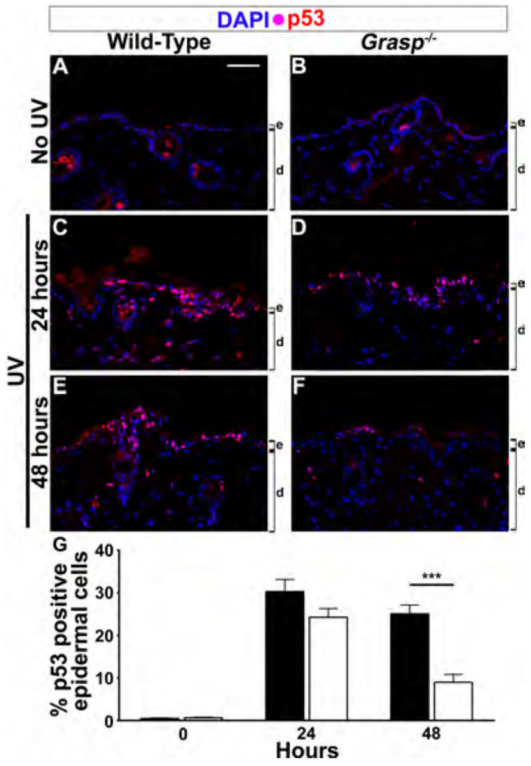

Fig. 6.

Aberrant nuclear localization of p53 in *Grasp*$^{-/-}$ mice after UVB exposure. (A–F) Immunohistochemical staining for p53 (red) in skin samples obtained at indicated time intervals after UVB exposure. Samples were counterstained with nuclear marker DAPI (blue). (G) Quantification and comparison of the p53+ cells of the epidermal basal layer at indicated times intervals following UVB exposure. Values in (G) represent the mean ± S.E.M. of three *Grasp*$^{-/-}$ mice and littermate controls for each time point. Statistical significance is indicated by *** for $p < 0.001$. Scale bars, 50 μM.